Ecological Indicators 167 (2024) 112717

Contents lists available at ScienceDirect

Ecological Indicators

journal homepage: www.elsevier.com/locate/ecolind

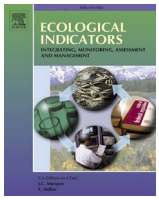

Original Articles

Distinct environmental controls on above- and below-ground net primary productivity in Northern China's grasslands

Haojun Zheng [a,f], Xiaofan Yang [b,c], Changqing Song [b], Wen Zhang [a], Wenjuan Sun [d], Guocheng Wang [a,b,c,e,*]

[a] LAPC, Institute of Atmospheric Physics, Chinese Academy of Sciences, Beijing 100029, China
[b] Faculty of Geographical Science, Beijing Normal University, Beijing 100875, China
[c] State Key Laboratory of Earth Surface Processes and Resource Ecology, Beijing Normal University, 100875, China
[d] State Key Laboratory of Vegetation and Environmental Change, Institute of Botany, Chinese Academy of Sciences, Beijing 100093, China
[e] Center for Geodata and Analysis, Beijing Normal University, Beijing 100875, China
[f] College of Earth and Planetary Sciences, University of Chinese Academy of Sciences, Beijing 100029, China

ARTICLE INFO

Keywords:
NPP
Remote sensing
Grasslands
Machine-learning model
Mapping
Northern China

ABSTRACT

Grasslands, which cover approximately 40 % of the global land surface, are crucial to the global carbon cycle due to their substantial carbon storage capacity and sensitivity to environmental changes. Net primary productivity (NPP) serves as a critical indicator of ecological function, representing the net carbon input to terrestrial ecosystems. Accurately quantifying and understanding grassland NPP, particularly below-ground net primary productivity (BNPP), and its responses to environmental changes are essential for assessing carbon sequestration potential and predicting future dynamics under varying environmental conditions. However, this remains challenging at large spatial scales. In our study, we integrated observations of above-ground net primary productivity (ANPP) with satellite-derived total net primary productivity (MODIS NPP) products across 508 individual locations in the diverse grasslands of Northern China. Plot-level BNPP was derived by subtracting field-measured ANPP from MODIS NPP and has been rigorously validated using field-measured BNPP from 68 ground sites. We then explored how climate, soil characteristics, topography, and grassland types influence ANPP and BNPP using machine learning models. Our results indicate that ANPP and BNPP averaged 154 g m^{-2} and 273 g m^{-2}, respectively, exhibiting significant variations across different grassland types. Furthermore, national mapping revealed regional disparities, with higher ANPP and BNPP values in the northeast compared to the southwest of Northern China. Climate was identified as the predominant driver of ANPP, explaining 41 % of the variance, followed by topography (26 %) and soil conditions (25 %). Conversely, topography had the most substantial impact on BNPP, accounting for 44 % of the explained variance, with climate and soil each contributing 25 %. These findings underscore the vulnerability of ANPP to climate change impacts such as droughts and temperature increases, and highlight how landscape features, such as elevation, slope, and aspect significantly influence BNPP, with crucial implications for soil carbon inputs and sequestration. Overall, this comprehensive study advances our understanding of the spatial patterns and environmental determinants of ANPP and BNPP in Northern China's grasslands. It offers valuable insights for developing sustainable management practices and for the preservation and effective management of these crucial ecosystems, especially in the context of ongoing environmental changes.

1. Introduction

As a critical component of the terrestrial ecosystems, grasslands are widely distributed, covering approximately 40 % of the global land surface (O'Mara, 2012). Grasslands not only provide numerous services, including food and bioenergy production and biodiversity conservation, but also serve as a vast carbon pool, accounting for 34 % of global terrestrial carbon stocks (White, 2000). In China, grasslands occupy about 40 % of the nation's total land area (Wang et al., 2011). However, due to the combination of climatic and anthropogenic factors,

* Corresponding author at: Faculty of Geographical Science, Beijing Normal University, Beijing 100875, China.
E-mail address: wanggc@bnu.edu.cn (G. Wang).

https://doi.org/10.1016/j.ecolind.2024.112717
Received 23 February 2024; Received in revised form 13 June 2024; Accepted 6 October 2024
Available online 12 October 2024

approximately 90 % of China's natural grasslands are experiencing degradation, with one of the main manifestations being the reduction in plant productivity (Pan et al., 2021). Grassland plant productivity is sensitive to factors such as climate, soil moisture, and nutrients, and its changes directly affect grassland carbon storage. Therefore, a thorough understanding of grassland productivity and its response mechanisms to environmental changes is crucial for formulating effective grassland conservation and management strategies and maintaining the carbon storage of grassland ecosystems.

Net primary productivity (NPP), the sum of above-ground (ANPP) and below-ground net primary productivity (BNPP), represents the net amount of carbon that plants capture through photosynthesis during a given period and serves as a crucial indicator of ecological functions (Lal et al., 2018; Sha et al., 2022). Whereas ANPP represents the carbon stored in aboveground plant parts, BNPP contributes significantly to soil carbon (Friedlingstein et al., 2022). Despite constituting more than 60 % of NPP in grasslands (Jackson et al., 2017; Wang et al., 2023), BNPP is one of the most uncertain and poorly understood carbon components in terrestrial ecosystems (Sha et al., 2022; Sun et al., 2023). This uncertainty stems from several factors. Firstly, BNPP estimation primarily relies on root growth measurements (Davidson et al., 2002; Garnier, 1991), which neglects the contribution of rhizodeposits, potentially resulting in underestimation (Gherardi and Sala, 2020). Secondly, measuring BNPP normally involves the labor-intensive and time-consuming process of extracting soil cores and separating roots from soil particles, which is prone to errors and biases. Furthermore, measuring BNPP without changing soil micro-environments, such as moisture, temperature, and nutrient availability, presents significant challenges.

Recently, Gherardi and Sala (2020) proposed an inverse estimation approach that combines field measurements of ANPP, satellite-derived total NPP, and climatic predictors to estimate BNPP globally. This method provides a reasonable estimation of BNPP without direct measurements (Gherardi and Sala, 2020). However, global-scale mapping results often suffer from uncertainties due to limited observation sites and uneven distribution across different biomes and regions (Wang et al., 2020; Zhao et al., 2005). A specific limitation in the study by Gherardi and Sala (2020) was evident in China's grasslands, where only 12 ANPP measurements were recorded, predominantly concentrated in the eastern parts of Inner Mongolia. In contrast, regions like central and western Inner Mongolia and the Qinghai-Tibetan Plateau exhibited sparse observation data coverage. This underscores the critical need for more extensive ground observations that are both large in number and evenly distributed to enhance the accuracy of both national ANPP and BNPP quantifications.

To optimize computing resources, many global predictions of productivity at high spatial resolutions employ simplistic models that incorporate only a few readily accessible variables, such as mean annual temperature and precipitation (Del Grosso et al., 2008; Gherardi and Sala, 2020). However, growing evidence indicates that edaphic and topographic factors co-regulate plant productivity (Bukombe et al., 2022; Ontl et al., 2013), especially for the belowground proportion (i.e., BNPP), which largely depends on soil moisture and nutrient conditions (Sun et al., 2018; Xiao et al., 2007). Neglecting the influence of these factors may lead to significant biases in estimating plant productivity. Despite this, few efforts have been made to thoroughly assess the regulating effects of these environmental drivers on ANPP and BNPP at reasonably large spatial scales in China's grasslands.

In this study, we conducted a comprehensive analysis of Northern China's natural grasslands by integrating ANPP observation data sourced from 132 publications (Text S1). These observations were integrated with satellite-based total NPP products to calculate plot-level BNPP, subsequently undergoing validation against field-observed BNPP data obtained from ANPP sites reporting BNPP. By considering various environmental factors, including climate, soil, and topography, we investigated the influence of these variables on both ANPP and BNPP. Furthermore, we employed machine learning techniques to extrapolate ANPP and BNPP to national scales, enabling us to summarize these attributes across different grassland types and regions. The primary objectives of our study were twofold: 1) to comprehensively explore how climatic, edaphic, and topographical variables influence ANPP and BNPP, and 2) to provide a more accurate national-scale mapping product of ANPP and BNPP.

2. Materials and methods

To quantify ANPP and BNPP, we first integrated ANPP observations with MODIS NPP products across 508 sites in Northern China's diverse grasslands. We then employed a series of machine learning (ML) models to assess the impacts of environmental variables on ANPP and BNPP, and to facilitate regional mapping and uncertainty analysis of the predictions. The ML models included random forest (RF), extreme gradient boosting (XGBoost), generalized linear models (GLM), support vector machines (SVM), Bayesian regularized artificial neural networks (BRANNs), and lasso regression (LASSO). Following training and validation, we selected the RF model for further analysis, regional mapping, and uncertainty assessment, as it demonstrated the lowest root mean squared error. A flowchart was generated for better illustrating the methodology visually (Fig. S1). The detailed steps are elaborated in Sections 2.1–2.4.

2.1. Data compilation of field measurements of ANPP and BNPP

To construct a synthesis dataset, we searched Web of Science and Chinese Science Citation Database using the keywords of *aboveground biomass, productivity, production, China* and *grassland* (or *pasture*) during November 2022-March 2023, and collected peer-reviewed publications reporting ANPP measurements in Northern China's grasslands. A recently published dataset reporting net primary productivity (NPP) across global grasslands (Sun et al., 2023) was retrieved and used to obtain the most comprehensive observational data of ANPP. We ultimately obtained 132 studies (62 in English and 70 in Chinese; Text S1) by screening the searched publications using the following criteria: 1) natural grasslands were involved; 2) observation year was reported; 3) experimental locations with precise latitude and longitude coordinates were specified; 4) amount of annual aboveground biomass or aboveground primary productivity was reported; 5) grassland type was reported or can be extracted from Vegetation Atlas of China (Chinese Academy of Science, 2001) using recorded locations and 6) the recorded or determined grassland type must be one of these five types including alpine meadow, alpine steppe, meadow steppe, typical steppe and desert steppe. We finally obtained 1,450 ANPP observations from 508 sites, and 377 BNPP observations from 68 locations (Fig. 1). All ANPP and BNPP data are standardized to the unit of grams of dry matter per square meter (g dry matter m^{-2}). If the unit of the original data was in grams of carbon per square meter (g C m^{-2}), then it should be divided by 0.45 for conversion (Sun et al., 2023).

2.2. Satellite-derived NPP and quantification of BNPP

Following Gherardi and Sala (2020), satellite-derived NPP was obtained from the NASA Earth Observing System, which generates yearly estimates of global NPP at a spatial resolution of 1 km^2 derived from the Moderate-Resolution Imaging Spectroradiometer (MODIS). Previous studies have demonstrated that the MODIS NPP data agrees well with productivity observations from modeling and in-situ measurements (Gherardi and Sala, 2020; Liu et al., 2018; Turner et al., 2005). Consequently, this NPP product is reliable for the broad spatial scales in this study.

At each site with ANPP measurement, the total NPP was retrieved from the MODIS NPP product using the recorded locations and years of ANPP observations. Following the method of Gherardi and Sala (2020),

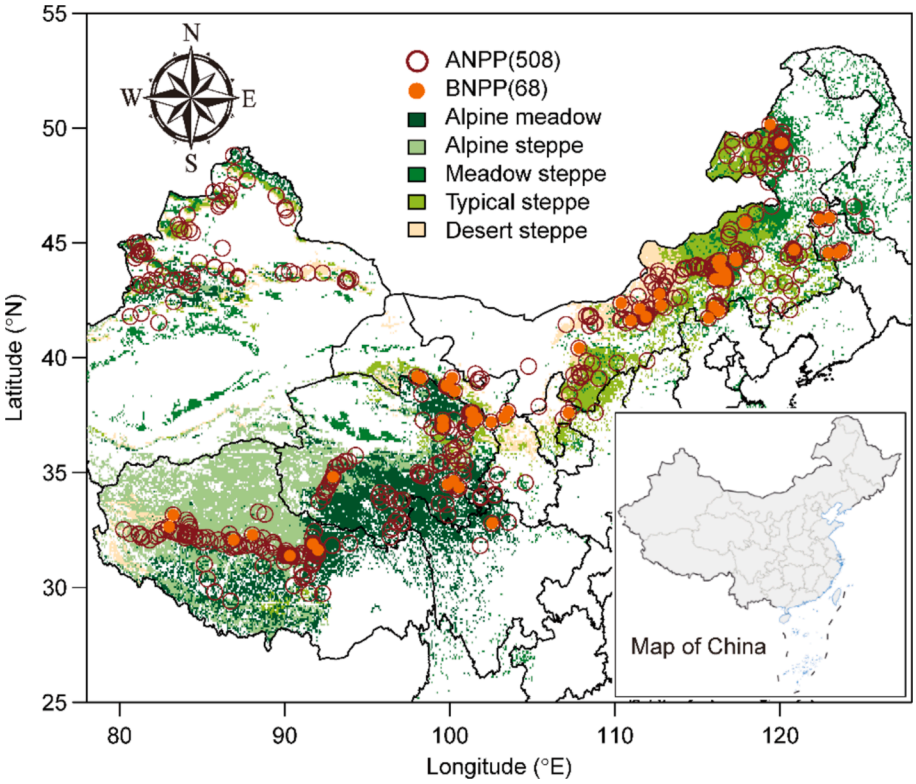

Fig. 1. Field measurements of above-ground (ANPP) and below-ground (BNPP) net primary productivity in Northern China's grasslands. Numbers in parentheses show total measurement locations.

plot-scale BNPP was estimated by subtracting ANPP from the satellite-derived NPP (i.e., MODIS NPP – ANPP). It is noteworthy that the MODIS NPP spans from 2001 to 2015. In cases where the ANPP observation year falls outside this specified time frame (which accounts for approximately 20 % of all ANPP measurements), we utilized the 15-year mean NPP as a substitute for the annual NPP of the corresponding year. It is essential to acknowledge that such discrepancies in the observation years between the field-measured ANPP and MODIS NPP may introduce potential uncertainties. However, these uncertainties are likely to have limited impacts on BNPP estimations for two primary reasons. Firstly, the majority of ANPP observations (approximately 80 %) align with the time frame of MODIS NPP. Secondly, the multi-year averaged MODIS NPP generally provides a reliable representation of NPP for a given location and has been widely employed to determine BNPP, either by multiplying NPP with f_{BNPP} (allocations of BNPP in total NPP) or by subtracting ANPP from NPP (Gherardi and Sala, 2020; Luo et al., 2020).

We proceeded to compare the indirectly derived BNPP, calculated by subtracting field-measured ANPP from MODIS-derived NPP, with the directly measured BNPP at field sites. The median BNPP values were 228 g m^{-2} and 240 g m^{-2} for the derived and measured BNPP, respectively (Fig. S2). Notably, the measured BNPP had considerably larger uncertainty, quantified by the deviation, compared to the derived BNPP (Fig. S2). Our findings confirm that the indirectly derived BNPP is comparable to the directly measured BNPP at field sites (Gherardi and Sala, 2020). Given the considerably larger sample size and lower uncertainty of the derived BNPP (Fig. S2), we opted to utilize it for our national mapping efforts (see Section 2.4).

2.3. Assessing impacts of environmental drivers on ANPP and BNPP

We collected regional environmental covariate layers, including climatic, edaphic, and topographic variables, to examine their impact on ANPP and BNPP (Section 2.3) and perform regional mapping (Section 2.4). We obtained a comprehensive dataset comprising 20 soil physiochemical properties (refer to Table S1 for indices and detailed descriptions) at a spatial resolution of 1 km^2 from the ISRIC-WISE soil profile database (Batjes, 2016). The WISE soil dataset encompasses seven layers, ranging from the topsoil (0–20 cm) to the bottom soil (150–200 cm), with our focus primarily on the topsoil layer. Furthermore, we derived 16 topographic attributes (refer to Table S1 for indices and detailed descriptions) from a global topography dataset with a spatial resolution of 1 km^2 (Amatulli et al., 2018). Additionally, we computed 19 plot-scale bioclimatic variables (refer to Table S1 for indices and detailed descriptions) based on monthly temperature and precipitation data corresponding to the year of ANPP observation. These bioclimatic covariates, derived from annual monthly temperature and precipitation data sourced from Peng et al. (2019), are ecologically significant (Fick and Hijmans, 2017). For national mapping, we acquired global gridded bioclimatic data at a 1 km^2 resolution from WorldClim (Fick and Hijmans, 2017). It is worth noting that the WorldClim database, released in 2020 and representing the period of 1970–2000, is widely recognized for its reliability and consistency across various geographical regions (Cook-Patton et al., 2020; Wadoux et al., 2020; Wang et al., 2023).

To analyze the spatial variability and responses of ANPP and BNPP to environmental drivers, we developed machine learning-based models. We retrieved environmental covariates using the geographic coordinates of ANPP measurements and fitted separate models for ANPP and BNPP. The models included random forest (RF), extreme gradient boosting (XGBoost), generalized linear models (GLM), support vector machines (SVM), Bayesian regularized artificial neural networks (BRANNs), and lasso regression (LASSO). Categorical variables were converted to dummy variables, and variables with high multicollinearity were excluded. The models were trained and validated using stratified samples, resulting in six models for each dependent variable. The model with the smallest root mean squared error was selected for further analysis and regional mapping.

The machine learning models we fitted provide insight into the

importance of predictor variables in predicting the dependent variables. For instance, the random forest (RF) model evaluates the importance of each predictor variable based on its impact on predictive accuracy (Cutler et al., 2007; Qi, 2012). The importance score is computed by evaluating the extent to which the impurity within the model decreases when it makes decisions to split the data based on the values of a particular variable. By averaging the decrease in impurity over all trees, the algorithm estimates the relative influence of each variable, with a scaled sum of 100 for ease of interpretation. We compared the overall relative influences of edaphic, bioclimatic, and topographic variables. Additionally, we conducted partial dependence analysis to determine the marginal effect of the five most important variables on ANPP and BNPP, while accounting for the average effect of other variables (Friedman and Meulman, 2003; Greenwell et al., 2018). This analysis was performed using the partial function in the R package *pdp*.

2.4. Regional mapping and prediction uncertainty of ANPP and BNPP

We utilized the fitted machine learning model with the smallest RMSE (i.e., RF model) to map ANPP and BNPP in Northern China's grasslands at a spatial resolution of 1 km^2. The model was run in each 1-km^2 pixel using environmental covariates extracted from the environmental data layers (see Section 2.3). Climatic, edaphic, and topographic predictors were set as numeric variables in the model simulations, while grassland type was treated as a categorical variable. The information of regional grassland type was derived from the Vegetation Atlas of China (Chinese Academy of Science, 2001). To predict the mean and uncertainty of ANPP and BNPP, we adopted a Monte Carlo approach. Specifically, we randomly drew 500 individual trees with replacement from the machine learning model. The 500 model-predicted estimates were used to determine the mean and standard deviation of the dependent variable at each pixel. The prediction uncertainty (U) was expressed as the coefficient of variation (CV), which is the standard deviation divided by the mean. All data analyses and figure productions were conducted in R 4.2.3 (R Development Core Team, 2023).

3. Results

3.1. NPP and its above- and below-ground allocations at site-levels

Averaged across 508 sites in Northern China's grasslands (Fig. 1), the total net primary productivity (NPP) is 441 g m^{-2} of dry matter, with a 95 % confidence interval (CI) ranging from 41 to 787 g m^{-2} (Fig. 2a). NPP varies significantly among grassland types, with alpine meadow having the highest NPP (571 g m^{-2}), followed by typical steppe (459 g m^{-2}) and meadow steppe (449 g m^{-2}). Meanwhile, alpine steppe has the lowest NPP (207 g m^{-2}), while desert steppe has the second lowest (247 g m^{-2}) (Fig. 2a). The study sites show an average ANPP of 154 g m^{-2} (95 %CI, 15–346 g m^{-2}) (Fig. 2b). Among grassland types, alpine meadow (186 g m^{-2}), meadow steppe (179 g m^{-2}), and typical steppe (162 g m^{-2}) have significantly higher ANPP than alpine steppe (89 g m^{-2}) and desert steppe (75 g m^{-2}) ($p < 0.05$).

On the other hand, BNPP across all sites is 273 g m^{-2}, with a 95 % CI extending from 11 to 571 g m^{-2} (Fig. 2c). Similar to the pattern observed for ANPP and NPP, BNPP is also relatively lower in alpine steppe (118 g m^{-2}) and desert steppe (173 g m^{-2}) compared to alpine meadow (335 g m^{-2}), meadow steppe (258 g m^{-2}), and typical steppe (297 g m^{-2}). The average proportional belowground allocation of NPP (f_{BNPP}) in Northern China's grasslands is 0.62, ranging from 0.20 to 0.92 (lower and upper bounds of 95 % CI, Fig. 2d). Across space, f_{BNPP} is generally higher in desert steppe (0.69) and typical steppe (0.64) than those in the remaining grassland types (0.53–0.59, Fig. 2d).

3.2. Drivers of above- and below-ground NPP

The results of model validation indicate that the machine learning-based models fitted well in capturing the variances in ANPP and BNPP, as evidenced by their R^2 values ranging from 0.46 to 0.69 and 0.55 to 0.74, respectively (Figs. 3 and 4). Among the six individual models, the random forest (RF) model has the best performance, demonstrated by its lowest root mean squared error (RMSE) and highest R^2 values in predicting both ANPP and BNPP (Figs. 3 and 4). As indicated by the fitted RF models, 69 % and 74 % of the variances in ANPP and BNPP, respectively, can be explained by predictors including

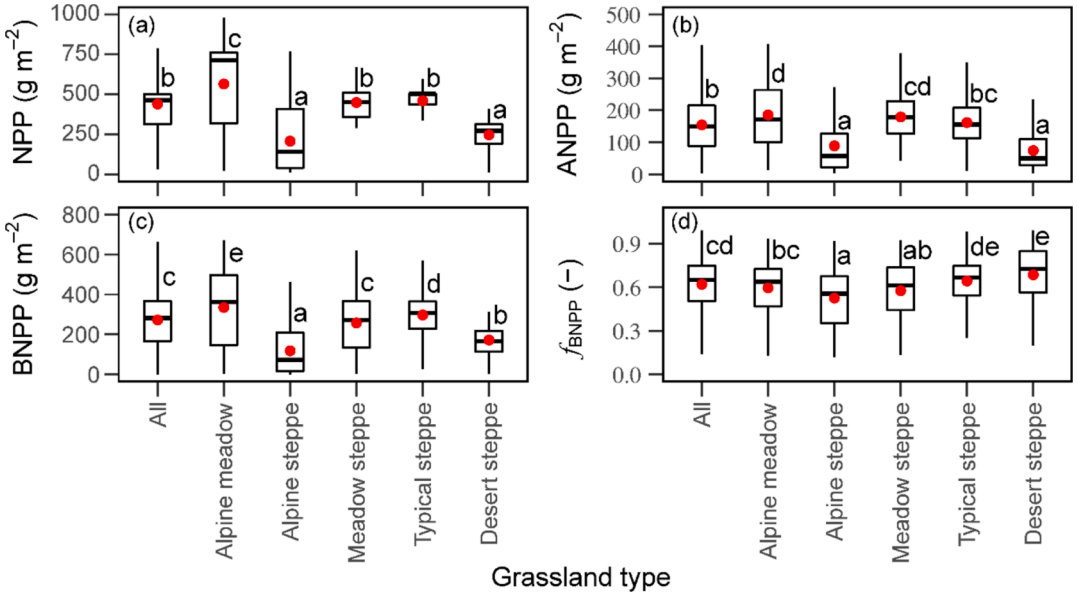

Fig. 2. Net primary productivity (NPP) and its components in Northern China's grasslands. The figure shows total NPP (a), above-ground (ANPP, b) and below-ground (BNPP, c) productivity and the fraction of BNPP to NPP (f_{BNPP}, d). ANPP are derived from field measurements (Fig. 1), NPP are retrieved from MODIS NPP product using the locations of ANPP measurements, and BNPP are calculated as the difference between NPP and ANPP. Red dots show the average, boxplots show the median and interquartile range with whiskers extending to 1.5 times the interquartile range. Different letters above the boxes indicate significant differences ($p < 0.05$). (For interpretation of the references to colour in this figure legend, the reader is referred to the web version of this article.)

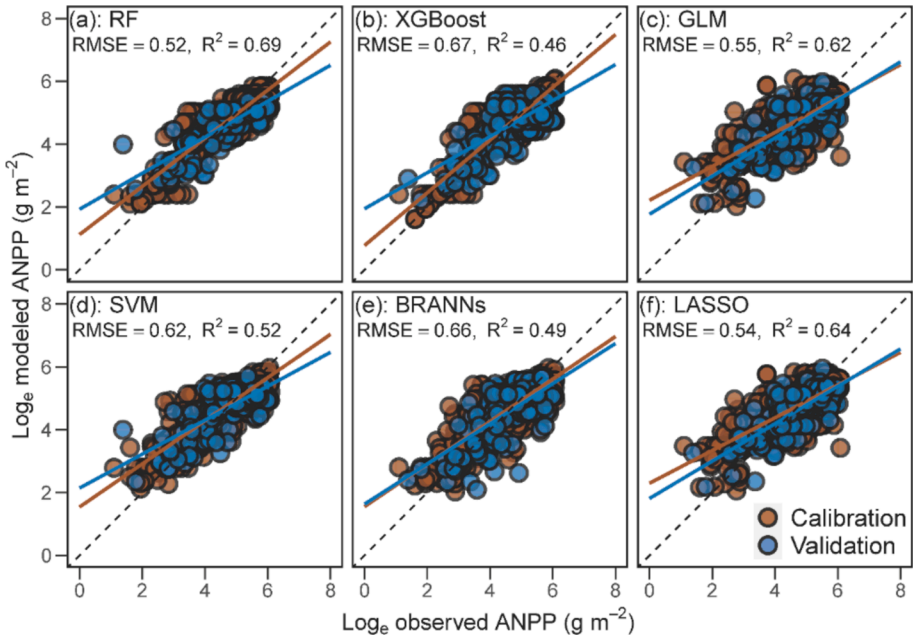

Fig. 3. Performance of machine learning models to predict above-ground net primary productivity (ANPP). a, random forest (RF); b, extreme gradient boosting (XGBoost); c, generalized linear models (GLM); d, support vector machines (SVM); e, Bayesian regularized artificial neural networks (BRANNs); f, lasso regression (LASSO). For each model, observations from randomly selected 80 % of the ANPP measurements are used for model calibration, with the data from the remaining 20 % for validation. RMSE and R^2 represent the rooted mean squared error and determination coefficient of validation, respectively.

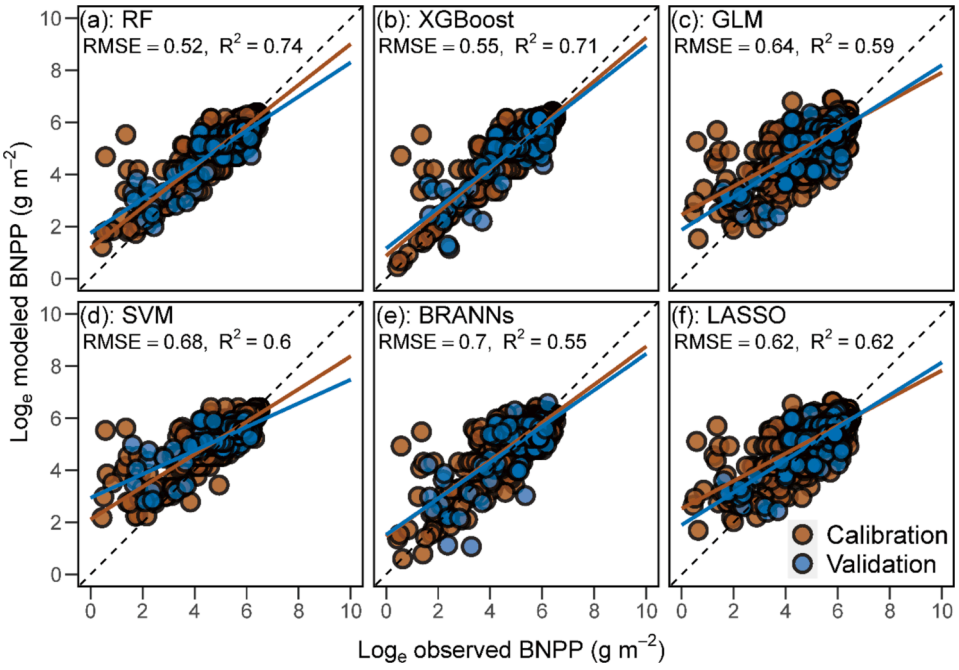

Fig. 4. Performance of machine learning models to predict below-ground net primary productivity (BNPP). BNPP are calculated as the difference between NPP, which are retrieved from a MODIS NPP product, and ANPP. a, random forest (RF); b, extreme gradient boosting (XGBoost); c, generalized linear models (GLM); d, support vector machines (SVM); e, Bayesian regularized artificial neural networks (BRANNs); f, lasso regression (LASSO). For each model, observations from randomly selected 80 % of the BNPP estimates are used for model calibration, with the data from the remaining 20 % for validation. RMSE and R^2 represent the rooted mean squared error and determination coefficient of validation, respectively.

climate, soil, topography and grassland type (Figs. 3a and 4a).

The results indicate that for ANPP, climate [represented mainly by P2 (precipitation of wettest month), T11 (mean temperature of coldest quarter), P4 (precipitation seasonality), T5 (max temperature of warmest month), T2 (mean diurnal range), and P3 (precipitation of driest month); see detailed descriptions in Table S1] is the most dominant regulator, alone explaining 41 % of the variance, followed by topography [26 %; indicated mainly by Elevation, VRM (vector ruggedness measure), Eastness (index from −1 to 1 of how east or west a site faces), Northness (index from −1 to 1 of how north a site faces), and Aspectsine (sine-transformed aspect)] and soil [25 %; represented mainly by GYPS (gypsum content), BSAT (base saturation), and ECEC

(effective cation exchange capacity)], while grassland type had marginal effects (Fig. 5a). Figure 5b shows the effects of the five most important variables controlling ANPP. ANPP generally increases with increasing P2 until reaching a plateau at relatively high P2 values, while it decreases with increasing elevation and T11.

On the other hand, for BNPP, topography (mainly indicated by Elevation, VRM, Northness, and Aspectsine) is the most dominant regulator, alone explaining 44 % of the variance, followed by climate (25 %; mainly represented by P2, T2, T11, T5, P4, and P3), and soil [25 %; mainly indicated by BSAT, CFRAG (coarse fragments), GYPS, and CECc (cation exchange capacity of clay size fraction)], while grassland type has limited effects (Fig. 5c). Elevation is the most individual important variable and has a negative effect on BNPP (Fig. 5d). In general, BSAT, VRM, and P2 have positive effects on BNPP (Fig. 5d).

3.3. Regional patterns of above- and belowground NPP and their prediction uncertainties

We utilized the independently tested models (Figs. 3a and 4a) along with covariates such as soil, climate, grassland type, and topography layers (Table S1) to digitally map ANPP and BNPP (Figs. 6a and 7a) and their respective uncertainties across the study area at a spatial resolution of 1 km^2 (Figs. 6b and 7b). The spatial distribution of ANPP varies significantly, ranging from less than 50 g m^{-2} to more than 200 g m^{-2} (Fig. 6a). The average ANPP across the study region is 112 g m^{-2}, with a 95 % CI ranging from 51 to 117 g m^{-2} (Table 1). ANPP generally decreases from the northeast to the southwest of the study region (Fig. 6a). On average, meadow steppe has the highest ANPP (147 g m^{-2}), followed by alpine meadow (110 g m^{-2}). In contrast, alpine steppe, typical steppe, and desert steppe have relatively lower average ANPP of ~ 100 g m^{-2} (Table 1). In addition, BNPP exhibits a spatial pattern similar to that of ANPP, i.e., relatively higher in the northeast than that in the southwest of the study region (Fig. 7a). The average BNPP across the study region is 193 g m^{-2}, with a 95 % CI ranging from 42 to 336 g m^{-2} (Table 1). Among grassland types, on average, meadow steppe and typical steppe have relatively higher BNPP (248–264 g m^{-2}) compared to other grassland types (120–192 g m^{-2}; Table 1).

The spatial variability in prediction uncertainty, quantified by the coefficient of variation (CV), is substantial for both ANPP and BNPP (Figs. 6b and 7b). On average, ANPP exhibits higher uncertainty in alpine steppe (with an average CV of 0.85) and typical steppe (0.82) compared to the other three grassland types (Table 1). For BNPP, alpine steppe has the highest uncertainty (1.11), followed by desert steppe (1.08) and alpine meadow (0.82). In contrast, meadow steppe and typical steppe exhibit relatively lower uncertainty of BNPP (Table 1).

4. Discussion and conclusion

ANPP is an important attribute studied in China's grasslands, commonly estimated through peak above-ground biomass (AGB) measurements (Prevéy and Seastedt, 2014). Previous studies in China have shown variations in AGB values across different grassland types (Ma et al., 2010a,b; Yang et al., 2010). Yang et al. (2010) conducted a comprehensive sampling across Northern China from 2001 to 2005, finding higher AGB values in meadow steppe (194 g m^{-2}), alpine meadow (100 g m^{-2}), and typical steppe (128 g m^{-2}) compared to alpine steppe (41 g m^{-2}) and desert steppe (60 g m^{-2}). These findings align with our results on ANPP in different grassland types in China (Fig. 2b and Table 1). The lower AGB reported by Yang et al. (2010) compared to our ANPP measurements can be attributed to their survey being conducted during the summer season, which may not represent the highest annual value (i.e., ANPP). Additionally, grazing activities can lead to a decrease in measured AGB compared to ANPP. Our regression analysis using a random forest model shows that precipitation during the wettest month (P2) has the greatest influence on ANPP (Fig. 5a and b). Meadow steppe and alpine meadow, with higher P2

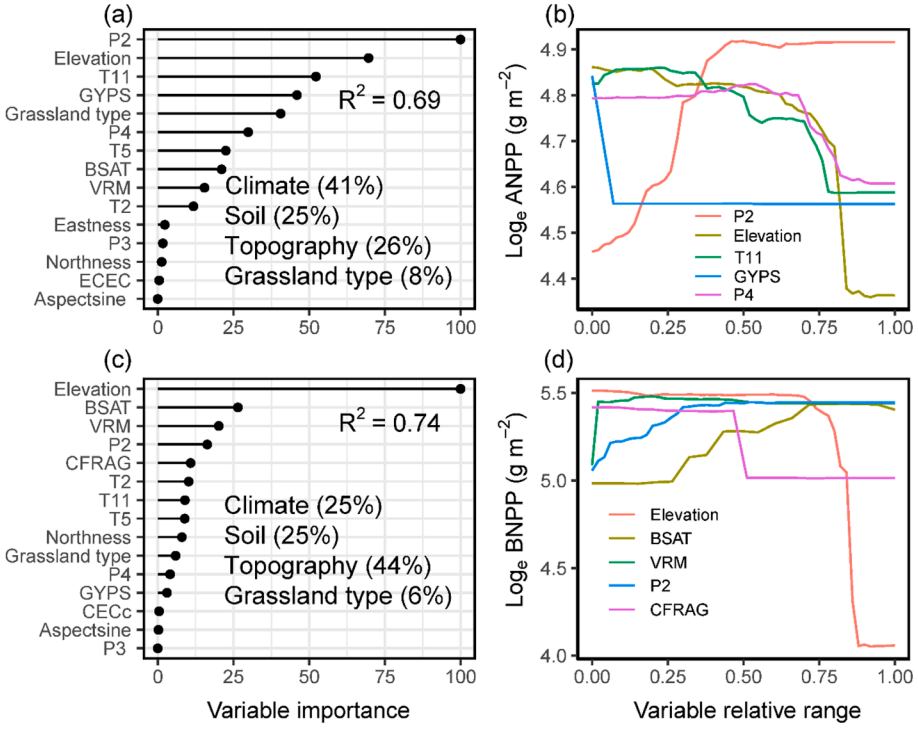

Fig. 5. Controls on above-ground (ANPP) and below-ground net primary productivity (BNPP) in Northern China's grasslands. The figure shows relative importance of predictor factors on ANPP (a) and relative importance of predictor factors on BNPP (c) based on random forest models. The predictors were selected by redundancy analysis to control variable collinearity and auto-correlation (see Table S1 for descriptions of all potential predictor variables). The figure also shows partial dependence plots of ANPP (b) and BNPP (d) on the five most important controls. Y-axes are logarithm-transformed and all x-axis variables are standardized from 0 to 1.

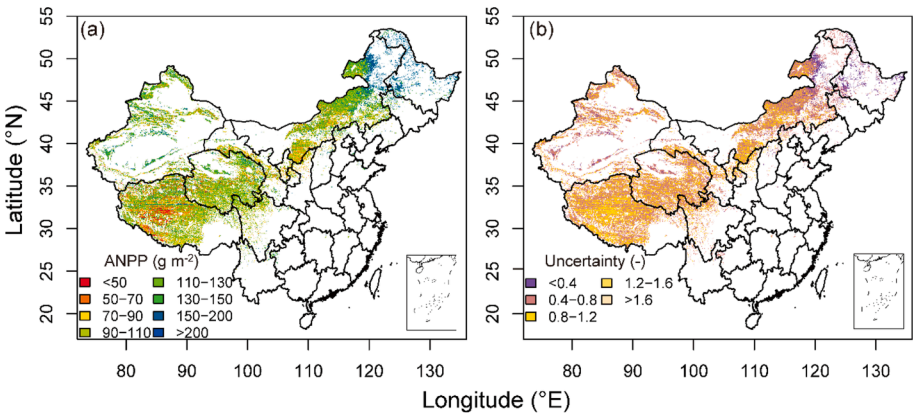

Fig. 6. Spatial pattern (a) and uncertainty (b) of above-ground net primary productivity (ANPP) in Northern China's grasslands. The RF model (Fig. 3a) is used to map spatial ANPP. Uncertainty is expressed as the margin of deviation of 500 Monte Carlo simulations divided by their mean, taking into account uncertainties in both observational data sets and prediction models.

Table 1
Above- (ANPP) and below-ground net primary productivity (BNPP) and their uncertainties indicated by regional mappings.

Grassland type	ANPP (g m^{-2})	Uncertainty of ANPP (−)[2]	BNPP (g m^{-2})	Uncertainty of BNPP (−)
All	112 (51, 117)[1]	0.77 (0.42, 1.12)	193 (42, 336)	0.79 (0.39, 1.71)
Alpine meadow	110 (68,159)	0.80 (0.58, 1.02)	192 (54, 350)	0.82 (0.47, 1.54)
Alpine steppe	98 (35, 162)	0.85 (0.60, 1.17)	120 (29, 303)	1.11 (0.58, 1.95)
Meadow steppe	147 (92, 186)	0.56 (0.38, 0.88)	264 (202, 332)	0.48 (0.35, 0.66)
Typical steppe	102 (56, 154)	0.82 (0.49, 1.17)	248 (195, 336)	0.52 (0.39, 0.73)
Desert steppe	105 (52, 158)	0.78 (0.57, 1.11)	125 (34, 334)	1.08 (0.50, 2.02)

[1] Average (the lower and upper bounds of the 95 % CI);
[2] Uncertainty was expressed as coefficient of variation (CV, standard deviation divided by the mean).

values, exhibit higher ANPP values compared to other grassland types (Table 1).

Measuring below-ground net primary productivity (BNPP) poses challenges due to the persistence of grassland plant roots over multiple years and the need to compare the highest and lowest below-ground biomass (BGB) values within a growing season (Davidson et al., 2002; Garnier, 1991). Consequently, comprehensive and high-quality BNPP datasets at large spatial scales are limited due to resource requirements (Le Quéré et al., 2018; Malhi et al., 2017). Our estimated BNPP, obtained by combining satellite-derived NPP with synthesized field measurements of ANPP, averages 273 g m^{-2}, which aligns with similar global estimates (Gherardi and Sala, 2020). Recent findings by Xiao et al. (2023) in global temperate grasslands also support our results, reporting an average BNPP of 321 g m^{-2} and highlighting the influence of edaphic, climatic, and topographic factors on BNPP (Fig. 5c and d). These findings indirectly validate the reliability of our study. We want to emphasize that the magnitude of the BNPP derived using MODIS NPP in combination with measured ANPP is, overall, comparable to that of the directly measured BNPP (Fig. S2). Here, it should be noted that in field measurements, BNPP can be assessed using various methods by different researchers, including root growth measurements (e.g., ingrowth cores) (Davidson et al., 2002; Garnier, 1991) or advanced tracer techniques (e.g., carbon isotopes) (Balesdent et al., 2018), potentially introducing significant uncertainties. Additionally, BNPP allocated to root exudates and mycorrhizae may constitute a substantial portion of BNPP but is challenging to measure in situ (Clark et al., 2001). Given the considerably large sample size and reduced uncertainty associated with the derived BNPP (Fig. S2), we have chosen to utilize it for national mapping.

The inferred below-ground net primary productivity (f_{BNPP}) represents 62 % of total net primary productivity (MODIS NPP) in our study, consistent with previous findings ranging from 54 % to 64 % (Gherardi and Sala, 2020; Jackson et al., 2017; Xiao et al., 2023). In arid

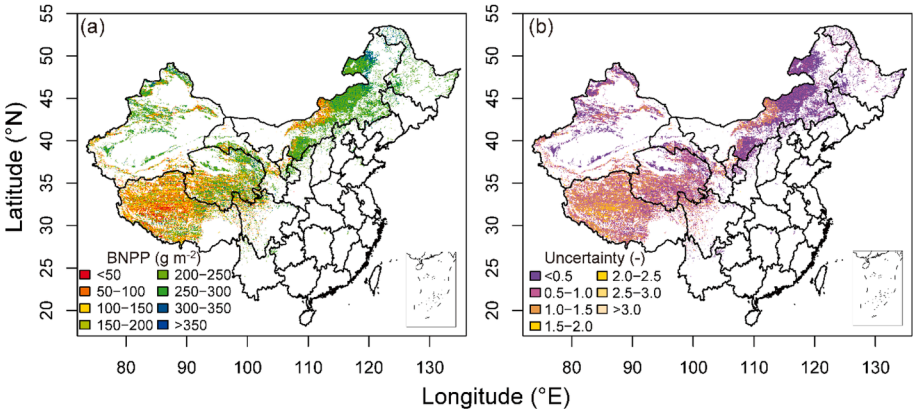

Fig. 7. Spatial pattern (a) and uncertainty (b) of below-ground net primary productivity (BNPP) in Northern China's grasslands. The RF model (Fig. 4a) is used to map spatial BNPP. Uncertainty is expressed as the margin of deviation of 500 Monte Carlo simulations divided by their mean, taking into account uncertainties in both observational data sets and prediction models.

environments like desert steppe and typical steppe, f_{BNPP} tends to exceed 60 %, while in other areas, it is relatively lower (below 60 %) (Fig. 2d). This pattern can be attributed to plants in arid regions developing deeper root systems to access water from lower soil layers, facilitating efficient water and nutrient absorption for optimized growth (Kirschner et al., 2021; Lynch, 1995). The depth and distribution of roots are influenced by unpredictable water availability in arid soils, with deeper layers receiving recharge from winter and spring precipitation (Ryel et al., 2004). This adaptation allows plants to cope with limited and uncertain water resources in arid regions (Ehleringer et al., 1991).

The machine learning models effectively captured variations in ANPP (Fig. 3) and BNPP (Fig. 4), with climate, soil, topography, and grassland type as significant predictors. Climate primarily regulated ANPP, while topography had the greatest influence on BNPP, followed by climate and soil (Fig. 5a and c). We further analyzed the longitudinal patterns of ANPP, BNPP, and their key influencing factors (Fig. S4). Along the longitudinal gradient, both ANPP and BNPP exhibited fluctuations, with BNPP consistently higher than ANPP (Fig. S4a). This finding aligns with the established understanding that BNPP constitutes more than 60 % of NPP in grasslands (Jackson et al., 2017; Wang et al., 2023). Additionally, we observed that regions with higher longitudes generally had higher ANPP and BNPP compared to those with lower longitudes (Fig. S4a). This pattern is related to the longitudinal variations in the five most important predictor factors identified by the machine learning models (Fig. S4b and c). ANPP is mainly governed by climate factors, especially precipitation, affecting photosynthesis and aboveground biomass production (Rustad et al., 2001; Wu et al., 2011). In contrast, a recent study by Gherardi and Sala (2020) showed that precipitation alone could only account for 36 % of the variance in BNPP globally. Our study demonstrated that incorporating topography and soil variables explained more than 70 % of the variance in BNPP (Fig. 4a). We also found that topography exerts the most significant influence on the derived BNPP, with climate and soil following closely (Fig. 5c). This alignment with the derived BNPP is consistent with the primary influence of topography on the measured BNPP, as indicated by the random forest model regression (Fig. S3). More specifically, topographical attributes such as Elevation, VRM (vector ruggedness measure), and Aspectsine (aspect sine) are consistently identified as influential factors for both datasets, namely derived and measured BNPP (Figs. 5c and S3a). Indeed, topography plays a crucial role in shaping belowground plant growth and root development by influencing soil properties, water movement, and vertical distribution (Ritchie et al., 2007; Schwanghart and Jarmer, 2011), ultimately affecting belowground plant growth and root development. Given the comparatively lesser impact of climate on BNPP in contrast to its influence on ANPP (Fig. 5) and the significant role of BNPP in contributing to soil carbon input (Wang et al., 2023), it is plausible to suggest that BNPP and soil carbon storage could exhibit greater stability in the face of a changing climate, including scenarios involving droughts and temperature increases. In addition, it is important to recognize that the influences of various factors on BNPP can vary depending on the scale and the specific biome. For instance, as demonstrated by Xiao et al. (2023), mean annual temperature and precipitation emerge as the two primary driving forces governing BNPP in nine major global biomes.

Several uncertainties should be acknowledged in terms of data and method qualities. Firstly, although previous studies have shown MODIS NPP aligned well with productivity observations derived from modeling and in-situ measurements, the integration of remote sensing data with field observations can introduce uncertainties arising from scale mismatches, temporal inconsistencies, and differences in measurement techniques. In future studies, the use of higher-resolution products that have undergone extensive ground validation and calibration can minimize the uncertainties associated with data integration. Secondly, the spatial representativeness of the selected grassland sites, particularly in remote regions like northern and southern Tibet (Fig. 1), may introduce uncertainties. Additional field observations are necessary to more comprehensively represent the study region. Thirdly, although machine learning-based models performed well in predicting ANPP and BNPP and capturing variance (Figs. 3 and 4), limitations and potential biases exist within these models. The accuracy of predictions depends on the quality and representativeness of the input data used for training. Lastly, due to data limitations, some important variables such as land management practices, grazing intensity, biodiversity levels, species composition, and disturbance regimes, which can significantly influence NPP dynamics, were not explicitly considered. According to the report by Fang et al. (2016), most of China's grasslands are natural, with a relatively small area of managed grasslands. The observational data used in this study were mainly derived from these natural grasslands and therefore did not include information on these variables. Future research should strive to collect and integrate more comprehensive data on these factors to better understand their impacts on grassland productivity dynamics.

Understanding grassland productivity and its response to environmental changes is crucial for the management and conservation of these ecosystems and for advancing our knowledge of the global carbon cycle. Despite the aforementioned uncertainties and limitations, this study provides valuable insights into the dynamics of NPP and its above- (ANPP) and below-ground (BNPP) allocations in Northern China's grasslands. Our findings reveal significant variability in ANPP and BNPP across grassland types, with climate being the most influential factor affecting ANPP, and topography having a major impact on BNPP. These insights are particularly valuable to policymakers and the scientific community, as they highlight the importance of climate and landscape features in regulating grassland productivity. For instance, the vulnerability of ANPP to climate change emphasizes the need for strategies that increase grassland resilience to extreme weather events. Meanwhile, the dominant role of topography on BNPP suggests that land management practices should consider local topographic conditions to enhance soil carbon sequestration. Furthermore, the regional differences in productivity revealed by our national mapping efforts can guide targeted approaches in grassland conservation, ensuring that management practices are adapted to the specific conditions of each region. By providing a detailed assessment of the spatial patterns and environmental drivers of grassland productivity, this study offers a robust framework for developing management practices that promote the sustainability and conservation of these vital ecosystems.

CRediT authorship contribution statement

Haojun Zheng: Writing – original draft, Visualization, Validation, Software, Methodology, Investigation, Formal analysis, Data curation. **Xiaofan Yang:** Writing – review & editing. **Changqing Song:** Writing – review & editing. **Wen Zhang:** Writing – review & editing. **Wenjuan Sun:** Writing – review & editing. **Guocheng Wang:** Writing – review & editing, Supervision, Project administration, Funding acquisition, Conceptualization.

Declaration of competing interest

The authors declare that they have no known competing financial interests or personal relationships that could have appeared to influence the work reported in this paper.

Data availability

All data used in this paper is publicly obtainable via this link: https://figshare.com/articles/dataset/NPP_and_its_above-_and_below-ground_allocations_in_China_s_grasslands/22657483.

Acknowledgments

This work was jointly supported by the National Natural Science

Foundation of China (Grant No. 42375116) and the Fundamental Research Funds for the Central Universities.

Appendix A. Supplementary data

Supplementary data to this article can be found online at https://doi.org/10.1016/j.ecolind.2024.112717.

References

Amatulli, G., Domisch, S., Tuanmu, M.-N., Parmentier, B., Ranipeta, A., Malczyk, J., Jetz, W., 2018. A suite of global, cross-scale topographic variables for environmental and biodiversity modeling. Sci. Data 5 (1), 1–15.

Balesdent, J., Basile-Doelsch, I., Chadoeuf, J., Cornu, S., Derrien, D., Fekiacova, Z., Hatté, C., 2018. Atmosphere-soil carbon transfer as a function of soil depth, 599-+ Nature 559 (7715). https://doi.org/10.1038/s41586-018-0328-3.

Batjes, N.H., 2016. Harmonized soil property values for broad-scale modelling (WISE30sec) with estimates of global soil carbon stocks. Geoderma 269, 61–68. https://doi.org/10.1016/j.geoderma.2016.01.034.

Bukombe, B., Bauters, M., Boeckx, P., Cizungu, L.N., Cooper, M., Fiener, P., Kidinda, L.K., Makelele, I., Muhindo, D.I., Rewald, B., Verheyen, K., Doetterl, S., 2022. Soil geochemistry – and not topography – as a major driver of carbon allocation, stocks, and dynamics in forests and soils of African tropical montane ecosystems. New Phytol. 236 (5), 1676–1690. https://doi.org/10.1111/nph.18469.

Chinese Academy of Science, 2001. Vegetation Atlas of China (in Chinese).

Clark, D.A., Brown, S., Kicklighter, D.W., Chambers, J.Q., Thomlinson, J.R., Ni, J., 2001. Measuring net primary production in forests: concepts and field methods. Ecol. Appl. 11 (2), 356–370. <Go to ISI>://WOS:000167876900004.

Cook-Patton, S.C., Leavitt, S.M., Gibbs, D., Harris, N.L., Lister, K., Anderson-Teixeira, K. J., Briggs, R.D., Chazdon, R.L., Crowther, T.W., Ellis, P.W., 2020. Mapping carbon accumulation potential from global natural forest regrowth. Nature 585 (7826), 545–550.

Cutler, D.R., Edwards Jr, T.C., Beard, K.H., Cutler, A., Hess, K.T., Gibson, J., Lawler, J.J., 2007. Random forests for classification in ecology. Ecology 88 (11), 2783–2792.

Davidson, E.A., Savage, K., Bolstad, P., Clark, D.A., Curtis, P.S., Ellsworth, D.S., Hanson, P.J., Law, B.E., Luo, Y., Pregitzer, K.S., Randolph, J.C., Zak, D., 2002. Belowground carbon allocation in forests estimated from litterfall and IRGA-based soil respiration measurements. Agric. For. Meteorol. 113 (1), 39–51.

Del Grosso, S., Parton, W., Stohlgren, T., Zheng, D., Bachelet, D., Prince, S., Hibbard, K., Olson, R., 2008. Global potential net primary production predicted from vegetation class, precipitation, and temperature. Ecology 89 (8), 2117–2126. https://doi.org/10.1890/07-0850.1.

Ehleringer, J.R., Phillips, S.L., Schuster, W.S., Sandquist, D.R., 1991. Differential utilization of summer rains by desert plants. Oecologia 430–434.

Fang, J., Bai, Y., Li, L., Jiang, G., Huang, J., Huang, Z., Zhang, W., Gao, S., 2016. Scientific basis and practical ways for sustainable development of China's pasture regions. Chin. Sci. Bull. 61 (2), 155–164.

Fick, S.E., Hijmans, R.J., 2017. WorldClim 2: new 1-km spatial resolution climate surfaces for global land areas. Int. J. Climatol.

Friedlingstein, P., Jones, M.W., O'Sullivan, M., Andrew, R.M., Bakker, D.C.E., Hauck, J., Le Quéré, C., Peters, G.P., Peters, W., Pongratz, J., Sitch, S., Canadell, J.G., Ciais, P., Jackson, R.B., Alin, S.R., Anthoni, P., Bates, N.R., Becker, M., Bellouin, N., Zeng, J., 2022. Global carbon budget 2021. Earth Syst. Sci. Data 14 (4), 1917–2005. https://doi.org/10.5194/essd-14-1917-2022.

Friedman, J.H., Meulman, J.J., 2003. Multiple additive regression trees with application in epidemiology. Stat. Med. 22 (9), 1365–1381.

Garnier, E., 1991. Resource capture, biomass allocation and growth in herbaceous plants. Trends Ecol. Evol. 6 (4), 126–131.

Gherardi, L.A., Sala, O.E., 2020. Global patterns and climatic controls of belowground net carbon fixation. Proc. Natl. Acad. Sci. 117 (33), 20038–20043.

Greenwell, B.M., Boehmke, B.C., McCarthy, A.J., 2018. A simple and effective model-based variable importance measure. arXiv preprint arXiv:1805.04755.

Jackson, R.B., Lajtha, K., Crow, S.E., Hugelius, G., Kramer, M.G., Piñeiro, G., 2017. The ecology of soil carbon: pools, vulnerabilities, and biotic and abiotic controls. Annu. Rev. Ecol. Evol. Syst. 48, 419–445.

Kirschner, G.K., Xiao, T.T., Blilou, I., 2021. Rooting in the desert: a developmental overview on desert plants. Genes 12 (5), 709.

Lal, R., Smith, P., Jungkunst, H.F., Mitsch, W.J., Lehmann, J., Nair, P.K.R., McBratney, A. B., Sa, J.C.D., Schneider, J., Zinn, Y.L., Skorupa, A.L.A., Zhang, H.L., Minasny, B., Srinivasrao, C., Ravindranath, N.H., 2018. The carbon sequestration potential of terrestrial ecosystems. J. Soil Water Conserv. 73 (6), A145–A152. https://doi.org/10.2489/jswc.73.6.145A.

Le Quéré, C., Andrew, R.M., Friedlingstein, P., Sitch, S., Pongratz, J., Manning, A.C., Korsbakken, J.I., Peters, G.P., Canadell, J.G., Jackson, R.B., 2018. Global carbon budget 2017. Earth Syst. Sci. Data 10 (1), 405–448.

Liu, L., Peng, S., AghaKouchak, A., Huang, Y., Li, Y., Qin, D., Xie, A., Li, S., 2018. Broad consistency between satellite and vegetation model estimates of net primary productivity across global and regional scales. J. Geophys. Res. Biogeo. 123 (12), 3603–3616.

Luo, Z., Luo, Y., Wang, G., Xia, J., Peng, C., 2020. Warming-induced global soil carbon loss attenuated by downward carbon movement. Glob. Chang. Biol. 26 (12), 7242–7254. https://doi.org/10.1111/gcb.15370.

Lynch, J., 1995. Root architecture and plant productivity. Plant Physiol. 109 (1), 7.

Ma, W., Fang, J., Yang, Y., Mohammat, A., 2010a. Biomass carbon stocks and their changes in northern China's grasslands during 1982–2006. Sci. China Life Sci. 53 (7), 841–850.

Ma, W., Liu, Z., Wang, Z., Wang, W., Liang, C., Tang, Y., He, J.-S., Fang, J., 2010b. Climate change alters interannual variation of grassland aboveground productivity: evidence from a 22-year measurement series in the Inner Mongolian grassland. J. Plant Res. 123 (4), 509–517. https://doi.org/10.1007/s10265-009-0302-0.

Malhi, Y., Girardin, C.A., Goldsmith, G.R., Doughty, C.E., Salinas, N., Metcalfe, D.B., Huaraca Huasco, W., Silva-Espejo, J.E., del Aguilla-Pasquell, J., Farfán Amézquita, F., 2017. The variation of productivity and its allocation along a tropical elevation gradient: a whole carbon budget perspective. New Phytol. 214 (3), 1019–1032.

O'Mara, F.P., 2012. The role of grasslands in food security and climate change. Annals of botany 110, 1263–1270.

Ontl, T.A., Hofmockel, K.S., Cambardella, C.A., Schulte, L.A., Kolka, R.K., 2013. Topographic and soil influences on root productivity of three bioenergy cropping systems [Article]. New Phytol. 199 (3), 727–737. https://doi.org/10.1111/nph.12302.

Pan, Q., Sun, J., Yang, Y., Liu, W., Li, A., Peng, Y., Xue, J., Xia, H., Huang, J., 2021. Issues and solutions on grassland restoration and conservation in China. Bull. Chinese Acad. Sci. (Chinese Version) 36 (6), 666–674.

Peng, S., Ding, Y., Liu, W., Li, Z., 2019. 1 km monthly temperature and precipitation dataset for China from 1901 to 2017. Earth Syst. Sci. Data 11 (4), 1931–1946. https://doi.org/10.5194/essd-11-1931-2019.

Prevéy, J.S., Seastedt, T.R., 2014. Seasonality of precipitation interacts with exotic species to alter composition and phenology of a semi-arid grassland. J. Ecol. 102 (6), 1549–1561.

Qi, Y., 2012. Random forest for bioinformatics. In: Ensemble Machine Learning: Methods and Applications. Springer, pp. 307–323.

R Development Core Team, 2023. R: a language and environment for statistical computing. R Foundation for Statistical Computing http://www.R-project.org.

Ritchie, J.C., McCarty, G.W., Venteris, E.R., Kaspar, T., 2007. Soil and soil organic carbon redistribution on the landscape. Geomorphology 89 (1–2), 163–171.

Rustad, L., Campbell, J., Marion, G., Norby, R., Mitchell, M., Hartley, A., Cornelissen, J., Gurevitch, J., Gcte-News, 2001. A meta-analysis of the response of soil respiration, net nitrogen mineralization, and aboveground plant growth to experimental ecosystem warming. Oecologia 126, 543–562.

Ryel, R.J., Leffler, A.J., Peek, M., Ivans, C., Caldwell, M., 2004. Water conservation in Artemisia tridentata through redistribution of precipitation. Oecologia 141, 335–345.

Schwanghart, W., Jarmer, T., 2011. Linking spatial patterns of soil organic carbon to topography—a case study from south-eastern Spain. Geomorphology 126 (1–2), 252–263.

Sha, Z., Bai, Y., Li, R., Lan, H., Zhang, X., Li, J., Liu, X., Chang, S., Xie, Y., 2022. The global carbon sink potential of terrestrial vegetation can be increased substantially by optimal land management. Commun. Earth Environ. 3 (1), 8. https://doi.org/10.1038/s43247-021-00333-1.

Sun, Y., Chang, J., Fang, J., 2023. Above- and belowground net-primary productivity: a field-based global database of grasslands. Ecology 104 (2), e3904. https://doi.org/10.1002/ecy.3904.

Sun, J., Ma, B., Lu, X., 2018. Grazing enhances soil nutrient effects: trade-offs between aboveground and belowground biomass in alpine grasslands of the Tibetan Plateau. Land Degrad. Dev. 29 (2), 337–348.

Turner, D.P., Ritts, W.D., Cohen, W.B., Maeirsperger, T.K., Gower, S.T., Kirschbaum, A. A., Running, S.W., Zhao, M., Wofsy, S.C., Dunn, A.L., 2005. Site-level evaluation of satellite-based global terrestrial gross primary production and net primary production monitoring. Glob. Chang. Biol. 11 (4), 666–684.

Wadoux, A.-M.-C., Minasny, B., McBratney, A.B., 2020. Machine learning for digital soil mapping: applications, challenges and suggested solutions. Earth Sci. Rev. 210, 103359.

Wang, S., Wilkes, A., Zhang, Z., Chang, X., Lang, R., Wang, Y., Niu, H., 2011. Management and land use change effects on soil carbon in northern China's grasslands: a synthesis. Agric. Ecosyst. Environ. 142 (3), 329–340. https://doi.org/10.1016/j.agee.2011.06.002.

Wang, G., Xiao, L., Lin, Z., Zhang, Q., Guo, X., Cowie, A., Zhang, S., Wang, M., Chen, S., Zhang, G., Shi, Z., Sun, W., Luo, Z., 2023. Most root-derived carbon inputs do not contribute to long-term global soil carbon storage. Sci. China Earth Sci. 66 (5), 1072–1086. https://doi.org/10.1007/s11430-022-1031-5.

Wang, X., Zhao, C., Müller, C., Wang, C., Ciais, P., Janssens, I., Peñuelas, J., Asseng, S., Li, T., Elliott, J., 2020. Emergent constraint on crop yield response to warmer temperature from field experiments. Nat. Sustain. 3 (11), 908–916.

White, R., 2000. Pilot analysis of global ecosystems: grassland ecosystems technical report.

Wu, Z., Dijkstra, P., Koch, G.W., Peñuelas, J., Hungate, B.A., 2011. Responses of terrestrial ecosystems to temperature and precipitation change: a meta-analysis of experimental manipulation. Glob. Chang. Biol. 17 (2), 927–942.

Xiao, C., Janssens, I.A., Liu, P., Zhou, Z., Sun, O.J., 2007. Irrigation and enhanced soil carbon input effects on below-ground carbon cycling in semiarid temperate grasslands. New Phytol. 174 (4), 835–846.

Xiao, L., Wang, G., Chang, J., Chen, Y., Guo, X., Mao, X., Wang, M., Zhang, S., Shi, Z., Luo, Y., Cheng, L., Yu, K., Mo, F., Luo, Z., 2023. Global depth distribution of

belowground net primary productivity and its drivers. Glob. Ecol. Biogeogr. https://doi.org/10.1111/geb.13705.
Yang, Y., Fang, J., Ma, W., Guo, D., Mohammat, A., 2010. Large-scale pattern of biomass partitioning across China's grasslands. Glob. Ecol. Biogeogr. 19 (2), 268–277. https://doi.org/10.1111/j.1466-8238.2009.00502.x.
Zhao, M.S., Heinsch, F.A., Nemani, R.R., Running, S.W., 2005. Improvements of the MODIS terrestrial gross and net primary production global data set. Remote Sens. Environ. 95 (2), 164–176.